ISSN 0029-3865

CNPq

CBPF - CENTRO BRASILEIRO DE PESQUISAS FÍSICAS

Notas de Física

CBPF-NF-023/94

June 1994

Relativistic Effects on the Electronic Structure and Bonding of $[Ir(CN)_5]^{3-}$

S.R. Nogueira* and Diana Guenzburger

Centro Brasileiro de Pesquisas Físicas, Rua Dr. Xavier Sigaud, 150, 22290-180, Rio de Janeiro/RJ, Brasil.

*Universidade Federal do Rio de Janeiro, Instituto de Física, Cidade Universitária, Ilha do Fundão, 21945, Rio de Janeiro, RJ, Brasil.

Abstract

Fully relativistic and non-relativistic molecular orbital calculations were performed for the covalent paramagnetic complex $[Ir(CN)_5]^{3-}$, employing the self-consistent Discrete Variational method, in the framework of density functional theory. Relativistic effects on the electronic structure and chemical bonding are discussed by comparison of relativistic and non-relativistic one-electron energy levels, populations and bond orders. The influence of relativistic effects on calculated absorption energies of the electronic spectrum is briefly assessed.

Key-words: Relativistic; Molecular orbital; Ir complex.

I Introduction

In heavy transition metal atoms, such as Ir, relativistic effects have a significant influence on the energy and shape of the orbitals. Among the best known effects are the contraction of the $s_{1/2}$ and $p_{1/2}$ orbitals, that penetrate the nucleus, the consequent expansion of the d and f orbitals, due to increased nuclear shielding, and the relativistic (spin-orbit) splitting of orbitals with $\ell > 0$. As the atom forms chemical bonds, such effects will affect the charge distribution and stability of the molecules, and therefore may not be disregarded [1].

The ligand CN forms bonds with transition metal atoms that are very covalent in nature, resulting in strong electronic delocalization. Added to this, the presence of a relativistic atom induces complex and interesting effects. Here we report a comparative study of non-relativistic and relativistic molecular-orbital calculations for the square-pyramidal covalent paramagnetic complex $[Ir(CN)_5]^{3-}$, in which Ir is in the unusual formal oxidation state +2. Such species has been obtained by irradiation of the hexacoordinated diamagnetic (Ir +3) complex with electrons or X-rays in solid alkali halide matrices. $[Ir(CN)_5]^{3-}$ is a low-spin complex with one unpaired electron occupying the HOMO (highest occupied molecular orbital); its electronic structure has been investigated by EPR spectroscopy [2].

Relativistic effects in molecules are usually treated in two ways. In semi-relativistic methods, direct relativistic terms such as the mass-velocity correction and the Darwin term are included in the hamiltonian and treated self-consistently, whereas the spin-orbit interaction is initially neglected and, in some cases, treated later as a perturbation [3, 4].

These methods utilize one-component wave functions, which corresponds to ignoring the small-components, and collapsing the large-component solutions of the Dirac equation into one. In such a framework, indirect nuclear shielding effects are difficult to assess [1]. On the other hand, methods in which the full Dirac equation is solved treat the spin-orbit interaction self-consistently, inasmuch as 4-component wave functions are employed [5, 6]. Among these, the fully relativistic Discrete Variational Method (RDVM) [6], based on density functional theory [7], allows the treatment of both direct and indirect effects without any approximations other than the local potential.

The non-relativistic Discrete Variational Method (DVM) and its relativistic extension were employed here to investigate the electronic structure and bonding in $[Ir(CN)_5]^{3-}$. In Section II we describe briefly the methods and give some details of the calculations; in Section III we present and discuss the results, including relativistic effects in electronic transitions. In Section IV we summarize our conclusions.

II Theoretical Method

II.a Non-relativistic

In the DVM method [8], the set of one-electron Kohn-Sham equations [7] are solved for the complex (in hartrees):

$$[-1/2\nabla^2 + V_c(\vec{r}) + V_{xc}(\vec{r})]\phi_i(\vec{r}) = \varepsilon_i\phi_i(\vec{r}) \qquad (1)$$

where the Coulomb potential $V_c(\vec{r})$ includes both the electron-nucleus attraction and electron-electron repulsion, and $V_{xc}(\vec{r})$ is the local exchange-correlation potential, which

we have chosen in the form derived by Hedin and Lundqvist [9]. $V_{xc}(\vec{r})$ is a functional of the electronic density $\rho(\vec{r})$, which is taken as a sum over the molecular orbitals $\phi_i(\vec{r})$ with occupation numbers n_i:

$$\rho(\vec{r}) = \sum_i n_i |\phi_i(\vec{r})|^2. \tag{2}$$

The molecular orbitals $\phi_i(\vec{r})$ are expanded on a basis of numerical symmetrized atomic orbitals χ^s_μ,

$$\phi_i(\vec{r}) = \sum_\mu \chi^s_\mu(\vec{r}) C^i_\mu. \tag{3}$$

The discrete variational method leads to the secular equations, solved self-consistently:

$$([H] - [E][S])[C] = 0, \tag{4}$$

where the matrix elements of the Hamiltonian matrix $[H]$ and overlap matrix $[S]$ are summations over a three-dimensional grid of points, with weights defined as the volume per point. The three-dimensional grid is chosen to be regular inside a sphere of radius equal to 2.5 a.u. around the transition element Ir, where a precise polynomial numerical integration is performed [10]; outside this sphere and around all the other atoms, a pseudorandom Diophantine point generator is used to provide the points [8]. The total number of points employed here was of the order of 13,000.

In order to facilitate the calculation of the electron-electron repulsion integral, a model potential is defined [11] by replacing the exact electronic charge density $\rho(\vec{r})$ by a model charge density $\rho_M(\vec{r})$, which is represented by a multicenter overlapping multipolar expansion

$$\rho(\vec{r}) \cong \rho_M(\vec{r}) \equiv \sum_j d_j \rho_j(\vec{r}), \tag{5}$$

with

$$\rho_j(\vec{r}) = \sum_\nu^I {}' \sum_m C^{\nu\lambda}_{\ell m} R_N(r_\nu) Y_{\ell m}(\hat{r}_\nu). \tag{6}$$

The index $j \equiv (I, \ell, \lambda, N)$ denotes a symmetry-equivalent set of atoms (I), a particular partial wave character (ℓ), a given independent basis function (λ) associated to a particular ℓ (if necessary) and a particular radial degree of freedom (N). The ν summation ($\sum'$) runs only over the atoms equivalent by symmetry to the atom ν. The symmetry coefficients $C^{\nu\lambda}_{\ell m}$ are chosen to produce functions which belong to the totally symmetric representation of the molecular point group (since $\rho(\vec{r})$ is a scalar), $Y_{\ell m}$ are the usual real spherical harmonics and r_ν is the radial coordinate relative to site ν. $R_N(r_\nu)$ are piecewise parabolic radial functions localized inside a radial range $r_N < r < r_{N+1}$, which allow a convenient analytical integration. In the calculations reported here, terms up to $\ell = 2$ centered on Ir, C and N were included; for each center, five radial functions were considered.

The coefficients d_j are obtained variationally by a least-squares fit to the "true" density $\rho(\vec{r})$, subject to the condition that the model density integrates to the total number of electrons. For the present calculations, the least-squares error was of the order of 0.03, for both relativistic and non-relativistic calculations.

Atomic basis functions in equation (3) were obtained from numerical self-consistent atomic density-functional calculations. For Ir, the basis functions included in the variational space were 4f, 5s, 5p, 5d, 6s and 6p. For C and N, all orbitals were included. All core orbitals not included in the variational space were orthogonalized to the valence basis functions in the first iteration and kept "frozen" subsequently. In order to reduce spurious effects of basis truncation the following procedure was adopted: to start the self-consistent procedure, the atoms are considered neutral and basis functions are generated for neutral atoms. After self-consistency is achieved for the complex, a Mulliken-type [12] population analysis is performed and the populations obtained are used to define new charges and configurations for the atoms. These populations are defined by dividing the overlap population with weights proportional to the coefficients [12]. New basis functions are generated for the atoms with the charges and configurations obtained. This procedure is repeated until the charges and configurations of the complex atoms are similar to those of the atoms generating the basis.

II.b Relativistic

The starting point of the relativistic DVM [6, 13] is the one-electron Dirac hamiltonian (in hartrees, $c = 137.037$):

$$h_D = c\tilde{\alpha}.[\vec{p} - (1/c)\vec{A}] + c^2(\tilde{\beta} - 1) + A_0, \tag{7}$$

where $\tilde{\alpha}$ and $\tilde{\beta}$ are the 4×4 Dirac matrices, $\vec{p}$ the momentum operator, and $(\vec{A}, A_0)$ a four-component vector potential describing external fields. By setting $\vec{A} = 0$ and $A_0 = V_c(\vec{r}) + V_{xc}(\vec{r})$, where $V_c(\vec{r})$ is the Coulomb potential and $V_{xc}(\vec{r})$ the local exchange-correlation potential as in equation (1), one gets the relativistic extension of the one-electron Kohn-Sham equations

$$(h_D - \varepsilon_i)\phi_i(\vec{r}, s) = 0, \tag{8}$$

where $\phi_i(\vec{r}, s)$ is a four-component Dirac spinor.

As in the non-relativistic case, the molecular orbitals $\phi_i(\vec{r}, s)$ are expanded on a basis of numerical symmetrized atomic orbitals $\chi^s_\mu(\vec{r}, s)$,

$$\phi_i(\vec{r}, s) = \sum_\mu \chi^s_\mu(\vec{r}, s) C^i_\mu. \tag{9}$$

The symmetrized orbitals $\chi^s_\mu(\vec{r}, s)$ are taken to be linear combinations of atomic fourth-order central-field Dirac spinors $\chi_{nkm}(\vec{r}, s)$ given by

$$\chi_{nkm}(\vec{r}, s) = \begin{bmatrix} r^{-1} P_{nk}(r) \mathcal{Y}_{km}(\theta, \phi, s) \\ i r^{-1} Q_{nk}(r) \mathcal{Y}_{-km}(\theta, \phi, s) \end{bmatrix} \tag{10}$$

and are constructed by using the projection operator technique as applied to the point double groups [6, 13]. In equation (10), $P_{nk}(r)$ and $Q_{nk}(r)$ are, respectively, the "large" and "small" components of the Dirac spinor and $\mathcal{Y}_{km}$ is a vector-coupled function of a spherical harmonic $Y^m_\ell(\theta, \phi)$ and a spin function $\xi_\sigma(s)$ [14]. The orbitals $\chi_{nkm}(\vec{r}, s)$ are

eigenfunctions of the total angular momentum squared j^2 and of its projection j_z with eigenvalues $j(j+1)$ and m, respectively, and are of given parity. The relativistic quantum number k is defined by

$$k = \begin{cases} \ell \quad if \quad j = \ell - 1/2 \\ -(\ell+1) \quad if \quad j = \ell + 1/2 \,, \end{cases} \tag{11}$$

which includes both j and the parity.

Once we have obtained a basis of relativistic symmetrized atomic orbitals, the RDVM method leads to secular equations exactly analogous to the non-relativistic expressions, Eq. (4). Atomic relativistic basis functions (Eq. (10)) were obtained from numerical self-consistent relativistic atomic density functional calculations. The basis functions used for Ir were $4f_{5/2}$, $4f_{7/2}$, $5s_{1/2}$, $5p_{1/2}$, $5p_{3/2}$, $5d_{3/2}$, $5d_{5/2}$, $6s_{1/2}$, $6p_{1/2}$ and $6p_{3/2}$. For C and N, all orbitals were kept in the variational space.

The numerical integration methods and the model potential used in the molecular relativistic calculations, as well as all the details of computations, are fully analogous to the non-relativistic case described in section II.a. The relativistic DVM employs non-relativistic Coulomb and exchange-correlation potentials, which do not include quantum-electrodynamical corrections. Relativistic effects, however, do not change significantly the structure of the potential and most of these effects can be identified with modifications in the kinetic part of the hamiltonian, spin-orbit splitting and mass-velocity correction term.

The relativistic symmetrized basis functions were obtained with the codes of Goodman and Ellis [13], based on an automatic procedure that necessitates as input only the molecular geometry.

III Results and Discussion

In order to investigate the relativistic effects in the electronic structure and chemical bonding of $[Ir(CN)_5]^{3-}$, we have performed relativistic and non-relativistic molecular orbital calculations. The interatomic distances, estimated by extrapolation of values known for other transition metal hexacyano complexes [15] taking into account the respective covalent radii, were taken as: Ir-C=2.00Å, C-N=1.15Å. The $[Ir(CN)_5]^{3-}$ complex ion is expected to have the square-pyramidal structure (symmetry point group C_{4v}) depicted in Figure 1. The Ir ion is expected to lie out of the plane of the equatorial ligands (see Fig. 1), as evidenced by EPR measurements of the superhyperfine interaction with the four equivalent equatorial nitrogens [16]. The angle CN(ax)-Ir-CN(eq.) was taken to be 97.7^0, which is the equilibrium value according to semi-empirical calculations [17]. Non-relativistic wave functions of $[Ir(CN)_5]^{3-}$ have been also employed in the investigation of EPR parameters [18].

In Table I are given the energies ε_i (of Eqs. (1) and (8)) of the deeper molecular orbitals derived from the 4f, 5s and 5p orbitals of Ir. Comparison of non-relativistic and relativistic energies shows clearly the relativistic contraction of the 5s and $5p_{1/2}$ orbitals, which results in considerably lower energies, as compared to non-relativistic. In contrast, the relativistic molecular orbitals derived from 4f expand due to increased nuclear shielding, and thus

the energies are higher. These core orbitals, which in the non-relativistic calculation constitute a very narrow band of only 0.2eV width, in the relativistic calculation form a much broader band of width 4.4eV, due mainly to spin-orbit splitting. One may also observe that the $5p_{1/2}$ level lies ~9eV deeper than $5p_{3/2}$, merging with the 4f band.

In Fig. 2 are shown the valence orbital energies ε_i for the non-relativistic and relativistic calculations, as defined in Eq. (1) and Eq. (8). The lowest-energy group of levels below -15eV correspond to orbitals localized on the C and N atoms; since relativistic effects for these atoms are not significant, there is practicaly no difference for these levels in the two calculations. This is true for all other levels localized mainly on the ligands.

The second group of levels correspond to occupied C-N orbitals showing significant mixture with Ir, as may be observed in detail in Table II; this is evidence of the strongly covalent nature of the Ir-CN bond. On top of these levels are the occupied antibonding levels (or "crystal field" levels) pertaining mainly to Ir 5d. The main differences between non-relativistic and relativistic calculations in this region are as follows. First, the relativistic calculation results in a larger number of levels, due to the change to double-group symmetry. Second, the bottom level $10a_1$ is pushed down in the relativistic calculation. As seen in Table II, $10a_1$ has a non-negligible 5s participation; in the corresponding relativistic orbital 16e' this is decreased, since the 5s energy is much lower (see Table I). The 5d participation is decreased significantly, due to the higher energy of the atomic 5d orbital; in contrast, there is a significant (8%) $6s_{1/2}$ participation. Since the atomic $6s_{1/2}$ level is much deeper than its non-relativistic counterpart, this and the smaller 5d participation results in the stabilization of 16e' relative to $10a_1$.

On the other hand, the occupied antibonding "crystal field" group of levels, 27e', 21e" and 22e", are placed at higher energies than the corresponding non-relativistic $3b_2$ and 12e. This is due to the destabilization of the $5d_{3/2}$ and $5d_{5/2}$ atomic orbitals.

The last occupied orbital with one unpaired electron $15a_1$ has almost the same energy as its relativistic counterpart 28e'. In Table III are given in detail the Mulliken-type populations of these orbitals. It is seen that the unpaired electron is strongly delocalized towards the ligands; this delocalization, however, is smaller in the relativistic calculation, in which the 5d population is increased.

The group of lowest energy virtual levels in both non-relativistic and relativistic calculations show strong mixture between Ir and CN levels. Although one level may be identified as the "crystal field" level ($9b_1$ or 28e") due to a very high 5d population, most of the other levels have significant Ir participation. This again is evidence of the complexity of the bond between a 5d metal and a covalent ligand. The 5d population in 28e" is much higher than in $9b_1$, again a consequence of the higher energy of the relativistic 5d orbitals.

In Table IV are given the Mulliken-type total populations. The charge on Ir is somewhat decreased in the relativistic calculation. The 6s population is significantly increased in the latter; the 6p is also increased, and the 5d is decreased. As the 6s energy is lowered in the relativistic calculation, its population in the complex may increase without loss of stability. The reverse is true in the case of 5d.

In Table V are shown the values of the bond orders (defined as the total overlap populations) for the Ir-C and C-N bonds. It is interesting to observe that there is a noticeable increase in the Ir-C bond order due to relativistic effects; the increase in the d-

s-p hybridization of Ir, dicussed above, is probably an important factor in this stabilization of the Ir-CN bond. As for the C-N bond order, it does not change by relativistic effects, in conformity with the small atomic numbers of these atoms.

According to Density Functional theory, many-electron effects are expected to be incorporated in the electronic structure, although a one-particle picture is maintained. In addition, the electronic relaxation that occurs when an electron changes orbital in an electronic transition may be taken into account by a transition state calculation [19]. However, here we will concern ourselves only with the lowest-energy "crystal field" $d \rightarrow d$ transitions, between levels with strong Ir 5d components; since these transitions involve orbitals with similar compositions, relaxation effects may be expected to be of less importance. In fact, test calculations have shown that the difference between transition energies calculated with a transition state and those obtained by merely calculating the energy difference between the one-electron levels may be expected to be of the order of 10% [18]; accordingly, the latter procedure was adopted.

In Table VI are given the calculated electronic transition energies for the lowest $d \rightarrow d$ transitions. No account is taken here of the transition intensities, and only doublet excited states are considered. To our knowledge, the optical spectrum of $[Ir(CN)_5]^{3-}$ has not been reported; however, the spectrum of the analogous complex $[Co(CN)_5]^{3-}$ has been measured in solution [20], and the bands observed have been interpreted with the aid of theoretical calculations [21].

According to the present non-relativistic calculations, the lowest-energy electronic transitions of $[Ir(CN)_5]^{3-}$ are expected to lie at somewhat higher energies than those observed for $[Co(CN)_5]^{3-}$. The lowest-energy transition ($19.6 \times 10^3 cm^{-1}$) is predicted to be $^2A_1 \rightarrow {}^2E$, the same as for the Co complex, where it is seen at $10.4 \times 10^3 cm^{-1}$ [20, 21]. However, relativistic effects decrease the energy of the corresponding transition of $[Ir(CN)_5]^{3-}$ to $16.0 \times 10^{-3} cm^{-1}$ (see Table VI). The other $d \rightarrow d$ transition to the orbital of the unpaired electron ($3b_2 \rightarrow 15a_1$) is also shifted to lower energies (27e'→28e'and 21e"→28e'). On the other hand, the transition from the level of the unpaired electron $15a_1$ to $9b_1$ has its energy increased in its relativistic counterpart (28e'→28e").

It should be kept in mind that the naïve "crystal field" picture of $d \rightarrow d$ transitions are only a simplification useful in analysing the spectra. As may be seen in Table II, the bands of highest-energy occupied levels and lowest-energy virtual levels contain many orbitals with significant 5d components, other than the levels considered in Table VI. Thus the classification in "crystal field" or charge-transfer (metal→ligand and ligand →metal) transitions is not very realistic, and a detailed investigation of the optical spectrum of $[Ir(CN)_5]^{3-}$ would involve considerable complexity.

IV Conclusions

The non-relativistic and relativistic Density Functional molecular-orbital calculations for $[Ir(CN)_5]^{3-}$ reveal relativistic effects in the electronic structure and bonding of this complex. Among these, we observed the increase of Ir 6s and 6p populations, and decrease of 5d, in the relativistic calculation. In the latter, the unpaired electron in the HOMO orbital is somewhat less delocalized to the ligands, and the bond-order of the Ir-CN bond

is increased, indicating that relativistic effects contribute to stabilize the metal-ligand bond. The lowest-energy $d \rightarrow d$ transitions are shifted relativistically to lower energies.

Figure Captions

Figure 1 – The square-pyramidal complex $[Ir(CN)_5]^{3-}$. Ir is at the center; the darker ligand atoms are C.

Figure 2 – Non-relativistic and relativistic molecular-orbital energies of $[Ir(CN)_5]^{3-}$.

Table Captions

Table I – Shallow core molecular-orbital energies of $[Ir(CN)_5]^{3-}$.

Table II – Mulliken-type population analysis of the valence molecular orbitals of $[Ir(CN)_5]^{3-}$. Only values for Ir atomic orbitals are given. In % of one electron.
a) Last occupied orbital, with one electron.

Table III – Population analysis (in % of one electron) of the orbital of the unpaired electron (HOMO) of $[Ir(CN)_5]^{3-}$. C_{ax} stands for axial C, C_{eq} for equatorial.

Table IV – Total populations and charges of $[Ir(CN)_5]^{3-}$.

Table V – Bond orders of $[Ir(CN)_5]^{3-}$.

Table VI – Calculated energies of $d \rightarrow d$ electronic transitions of $[Ir(CN)_5]^{3-}$.
a) $1eV=8.0655\times10^3 cm^{-1}$.

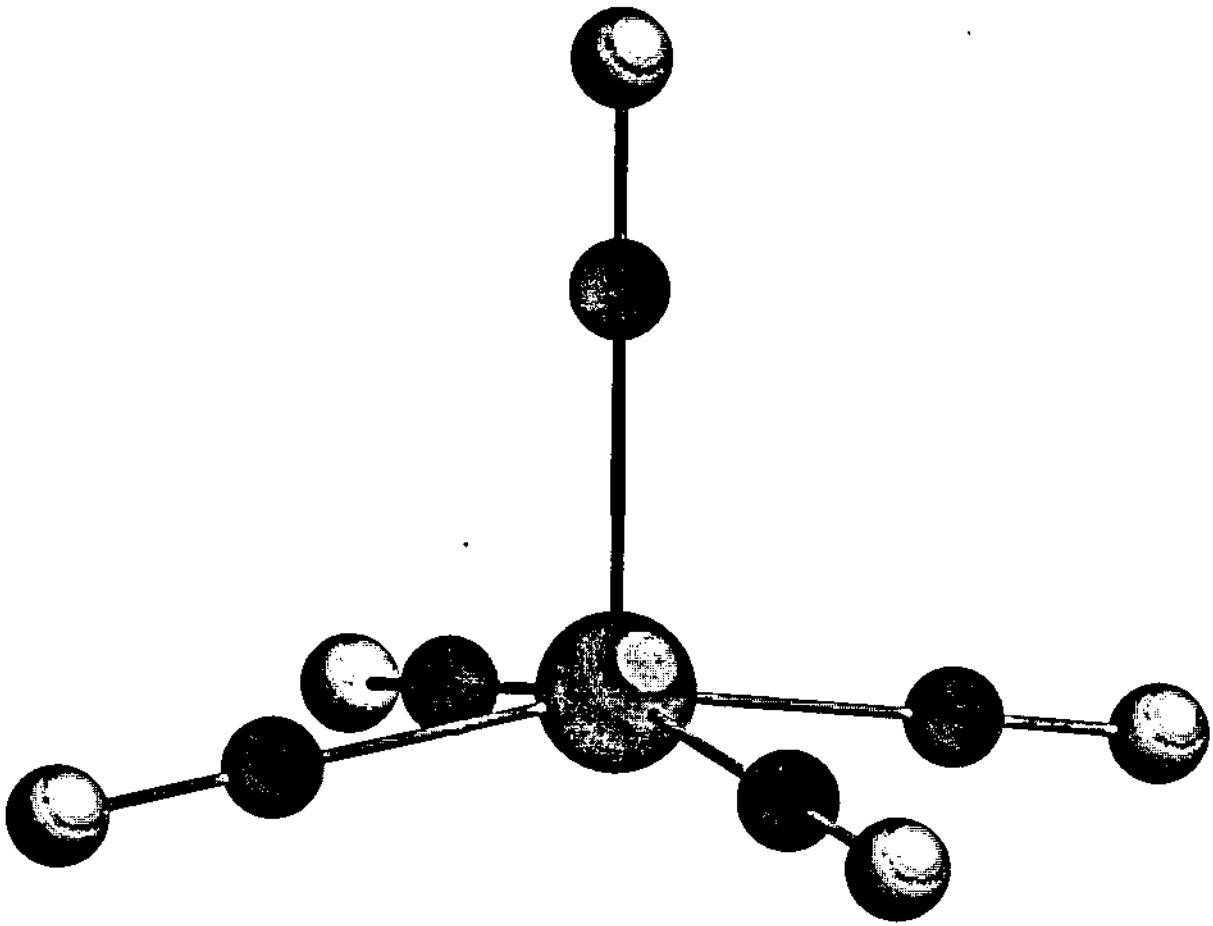

Fig. 1

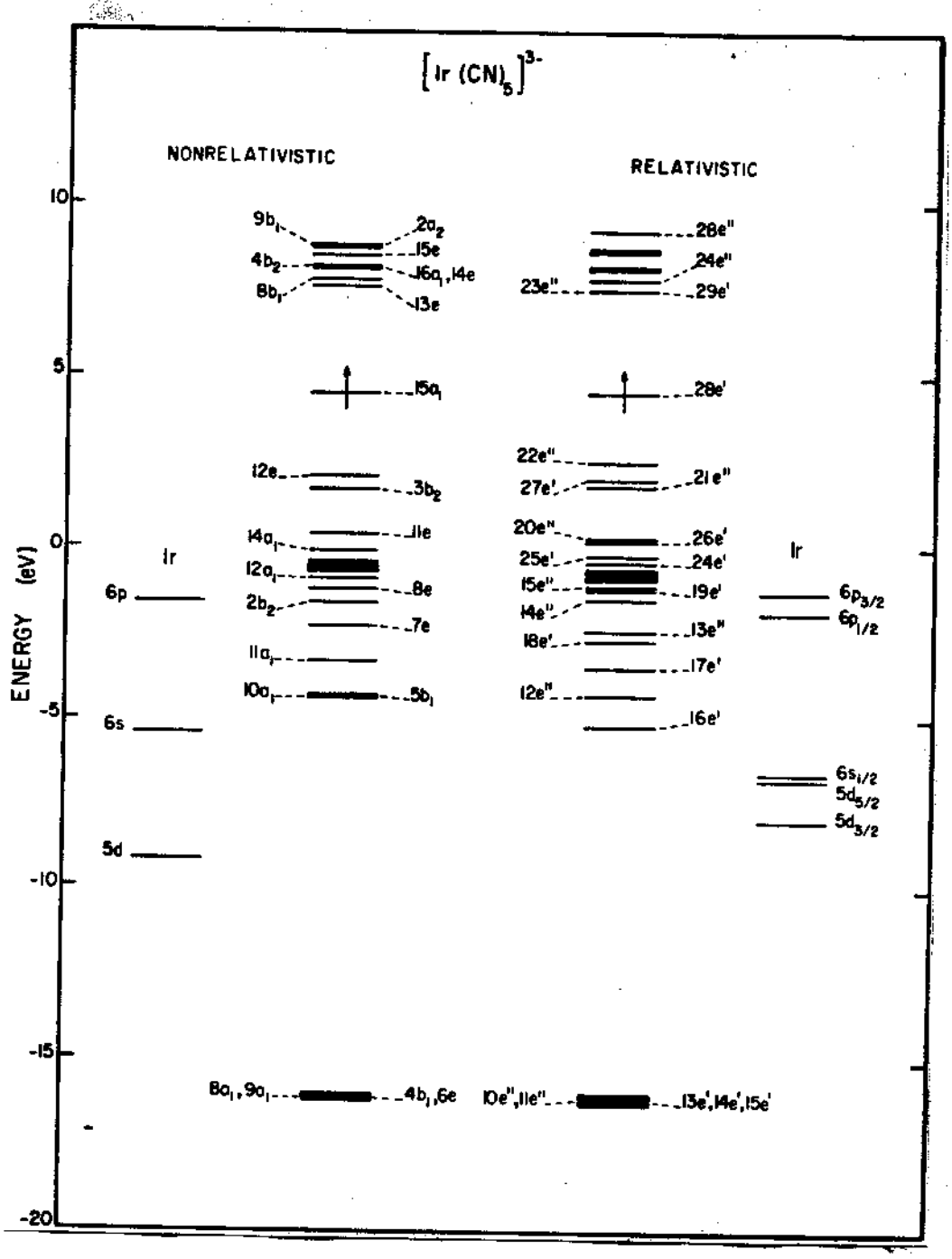
[Ir (CN)5]3-
NONRELATIVISTIC
RELATIVISTIC
ENERGY (eV)
10
5
0
-5
-10
-15
-20
Ir
6p
6s
5d
9b1
4b2
8b1
2a2
15e
16a1,14e
13e
15a1
12e
3b2
14a1
12a1
2b2
11a1
10a1
11e
8e
7e
5b1
8a1,9a1
4b1,6e
23e"
28e"
24e"
29e'
28e'
22e"
27e'
21e"
20e"
25e'
15e"
14e"
18e'
12e"
26e'
24e'
19e'
13e"
17e'
16e'
Ir
6p3/2
6p1/2
6s1/2
5d5/2
5d3/2
10e",11e"
13e',14e',15e'

Fig. 2

Table I

Non-relativistic			Relativistic		
Orbital	Enegy (eV)	Ir atomic character	Orbital	Energy (eV)	Ir atomic character
$5a_1$	-67.7	5s	7e'	-88.3	$5s_{1/2}$
3e	-62.5		8e'	-55.3	
$3b_1$	-62.4		5e"	-54.1	
$1b_2$	-62.4	4f	6e"	-54.1	$4f_{5/2}$,
4e	-62.4		9e'	-54.0	$4f_{7/2}$
$6a_1$	-62.3		10e'	-51.0	
			7e"	-50.9	
			8e"	-50.9	
5e	-40.1	5p	11e'	-50.9	$5p_{1/2}$
$7a_1$	-39.8		9e"	-41.8	$5p_{3/2}$
			12e'	-41.5	

Table II

Non-relativistic		Relativistic		Relativistic (cont.)	
Orbital	Composition	Orbital	Composition	Orbital	Composition
$10a_1$	3.9(5s), 11.3(5d)	16e'	$1.3(5s_{1/2}),7.5(6s_{1/2}),1.6(5d_{3/2}),\ 1.6(5d_{5/2})$	29e'	$1.5(6p_{1/2}),1.0(6p_{3/2})$
$5b_1$	44.8(5d)	12e"	$20.5(5d_{3/2}),19.4(5d_{5/2})$	23e"	$2.1(6p_{3/2})$
$11a_1$	1.2(5s),1.7(5p),16.0(5d)	17e'	$1.0(5p_{3/2}),10.8(5d_{3/2}),12.4(5d_{5/2})$	24e"	$2.2(5d_{3/2}),1.4(5d_{5/2})$
7e	2.5(5p),4.8(5d)	18e'	$4.0(5d_{3/2}),1.2(5p_{1/2}),1.0(5p_{3/2})$	30e'	$1.2(6s_{1/2}),8.4(5d_{3/2}),2.8(5d_{5/2})$
$2b_2$	23.2(5d)	13e"	$2.0(5p_{3/2}),1.0(5d_{3/2}),2.5(5d_{5/2})$	25e"	(C,N)
8e	16.1(5d)	14e"	$9.7(5d_{3/2}),11.9(5d_{5/2})$	31e'	$1.1(6s_{1/2}),4.5(5d_{3/2}),3.8(5d_{5/2})$
.....	.....	19e'	$11.0(5d_{3/2}),5.2(5d_{5/2})$	26e"	$13.3(5d_{3/2}),3.8(5d_{5/2})$
$12a_1$ to 10e···(C,N)		15e"	$1.4(5d_{3/2}),11.2(5d_{5/2})$	33e'	$1.0(6s_{1/2}),4.1(5d_{3/2}),11.7(5d_{5/2})$
.....	.....	.....	.....	33e'	(C,N)
$7b_1$	4.6(5d)	20e' to 18e"···(C,N)		27e"	$1.4(5d_{3/2}),18.0(5d_{5/2})$
$13a_1$	6.9(5d)	.....	.....	28e"	$12.5(5d_{3/2}),40.5(5d_{5/2})$
$14a_1$	3.3(6s),1.1(5d)	19e"	$2.0(5d_{3/2}),2.7(5d_{5/2})$		
11e	1.3(5p).4.9(6p),4.6(5d)	24e'	$2.2(5d_{3/2}),2.7(5d_{5/2})$		
$3b_2$	59.2(5d)	25e'	$2.5(6s_{1/2}),1.2(5d_{3/2}),1.2(5d_{5/2})$		
12e	3.9(6p),57.0(5d)	26e'	$5.4(6p_{1/2}),1.2(6p_{3/2}),$		
$15a_1^{(a)}$	3.1(6s),30.9(6p),27.8(5d)		$2.2(5d_{3/2}),1.0(5d_{5/2})$		
13e	1.5(6p)	20e"	$8.1(6p_{3/2}),2.4(5d_{5/2}),1.0(5d_{3/2})$		
$8b_1$	3.4(5d)	21e"	$31.0(5d_{3/2}),27.7(5d_{5/2})$		
$16a_1$	17.1(5d),1.9(6s)	27e'	$1.2(6p_{1/2}),2.5(6p_/3/2),$		
14e	1.1(5d)		$36.0(5d_{3/2}),22.5(5d_{5/2})$		
$4b_2$	22.2(5d)	22e"	$3.6(6p_{3/2}),3.1(5d_{3/2}),59.2(5d_{5/2})$		
15e	15.6(5d)	$28e'^{(a)}$	$3.4(6s_{1/2}),9.9(6p_{1/2}),$		
$2a_2$	(C,N)		$21.1(6p_{3/2}),8.1(5d_{3/2}),21.7(5d_{5/2})$		
$9b_1$	42.2(5d)				

Table III

Non-relativistic			Relativistic				
Ir	5s	0.0	Ir	$5s_{1/2}$	0.0		
	5p	0.6		$5p_{1/2}$	0.1	5p	0.3
	5d	27.8		$5p_{3/2}$	0.2		
	6s	3.1		$5d_{3/2}$	8.1	5d	29.8
	6p	30.9		$5d_{5/2}$	21.7		
C_{ax}		8.3		$6s_{1/2}$	3.4		
N_{ax}		3.3		$6p_{1/2}$	9.9	6p	31.0
C_{eq}(each)		3.7		$6p_{3/2}$	21.1		
N_{eq}(each)		2.8	C_{ax}		7.7		
			N_{ax}		3.1		
			C_{eq}(each)		2.7		
			N_{eq}(each)		3.4		

Table IV

Non-relativistic			Relativistic				
Ir	5s	1.94	Ir	$5s_{1/2}$	1.96		
populations:	5p	5.91	populations:	$5p_{1/2}$	1.98	5p	5.92
	5d	7.43		$5p_{3/2}$	3.94		
	6s	0.09		$5d_{3/2}$	3.17	5d	7.38
	6p	0.45		$5d_{5/2}$	4.21		
Charges:	Ir	+1.18		$6s_{1/2}$	0.23		
	C_{ax}	+0.07		$6p_{1/2}$	0.19	6p	0.51
	N_{ax}	-0.85		$6p_{3/2}$	0.32		
	C_{eq}	+0.02					
	N_{eq}	-0.87	Charges:	Ir	+1.01		
				C_{ax}	+0.08		
				N_{ax}	-0.84		
				C_{eq}	+0.05		
				N_{eq}	-0.86		

Table V

Non-relativistic		Relativistic
Ir-C_{ax}	0.30	0.48
Ir-C_{eq} (each)	0.31	0.48
C_{ax}-N_{ax}	1.36	1.36
C_{eq}-N_{eq} (each)	1.31	1.31

Table VI

Non-relativistic			Relativistic		
Transition		Energy[a] $(10^3 cm^{-1})$	Transition		Energy[(a)] $(10^3 cm^{-1})$
$3b_2 \rightarrow 15a_1$	$^2A_1 \rightarrow ^2B_2$	23.0	27e'→28e'	$^2E' \rightarrow ^2E'$	19.4
12e→15a_1	$^2A_1 \rightarrow ^2E$	19.6	21e"→28e'	$^2E' \rightarrow ^2E"$	21.8
$15a_1 \rightarrow 9b_1$	$^2A_1 \rightarrow ^2B_1$	34.7	22e"→28e'	$^2E' \rightarrow ^2E"$	16.0
			28e'→28e"	$^2E' \rightarrow ^2E"$	38.5

References

[1] a) P. Pyykkö, Adv. Quantum Chem. **11**, 353 (1978); b) M. Pepper and B.E. Bursten, Chem. Rev. **91**, 719 (1991); c) "Relativistic effects in atoms, molecules and solids", ed. G.L. Malli; Plenum Press, N. York (1981).

[2] N.V. Vugman, R.P.A. Muniz and J. Danon, J. Chem. Phys. **57**, 1297 (1972); N.V. Vugman and V.K. Jain, Rev. Roumaine Phys. **33**, 981 (1988).

[3] A. Goursot, H. Chermette and C. Daul, Inorg. Chem. **23**, 305 (1984).

[4] J.H. Wood and A.M. Boring, Phys. Rev. B **18**, 2701 (1978).

[5] J.P. Lopez and D.A. Case, J. Chem. Phys. **81**, 4554 (1984).

[6] A. Rosén and D.E. Ellis, J. Chem. Phys. **62**, 3039 (1975).

[7] R.G. Parr and W. Yang, "Density-functional theory of atoms and molecules", Oxford University Press, N. York (1989).

[8] D.E. Ellis and G.S. Painter, Phys. Rev. B**2**, 2887 (1970); D.E. Ellis, Int. J. Quantum Chem. **S2**, 35 (1968).

[9] L. Hedin and B.I. Lundqvist, J. Phys. C**4**, 2064 (1971).

[10] A.H. Stroud, "Approximate calculation of multiple integrals", Prentice Hall, Englewood Cliffs, N. Jersey (1971).

[11] B. Delley and D.E. Ellis, J. Chem. Phys. **76**, 1949 (1982).

[12] C. Umrigar and D.E. Ellis, Phys. Rev. B **21**, 852 (1980).

[13] D.E. Ellis and G.L. Goodman, Int. J. Quantum Chem. **25**, 185 (1984).

[14] I. Lindgren and A. Rosén, Case Sudies At. Phys. **4**, 93 (1974).

[15] J.J. Alexander and H.B. Gray, Coord. Chem. Rev. **2**, 29 (1967).

[16] N.V. Vugman, R.P.A. Muniz and J. Danon, J. Chem. Phys. **57**, 1297 (1972).

[17] S.R. Nogueira, N.V. Vugman and D. Guenzburger, Chem. Phys. **164**, 229 (1992).

[18] S.R. Nogueira and D. Guenzburger, unpublished.

[19] J.C. Slater, "The self-consistent field for molecules and solids", vol. 4, McGraw-Hill, N. York (1974).

[20] F.-D. Tsay, H.B. Gray and J. Danon, J. Chem. Phys. **54**, 3760 (1971).

[21] D. Guenzburger, A.O. Caride and E. Zuleta, Chem. Phys. Letters **14**, 239 (1972); A.O. Caride, H. Panepucci and S.I. Zanette, J. Chem. Phys. **55**, 3651 (1971).